# Responses to SSM on Radionuclide Transport

**Scott Painter, LANL, May 2013**

**SSM Question**: In TR-10-51 (section 3.10.1) it is stated that MARFA is a category 4b code. In section 2.3 of TR-10-51it is stated that the QA routines are: "4b. Calculations performed with codes developed within the safety assessment, frequently written in languages like C++ and Fortran. These codes are in general written with the safety assessment application in mind and have a considerably smaller user base than codes in category 3. The need for verification is thus larger for these codes." It is stated that "Software [verification] tests are summarized in the MARFA user's manual" (R-09-56), but this document contains errors as described in Robinson and Watson (2011). Appendix C in TR-10-50 presents a comparison between MARFA and FARF31. The comparison is based on a narrow application range and cannot be considered or assumed to be a check of MARFA to any greater extent. It may well be that the MARFA code is suitable for the types of applications considered in SR-Site, but there is a clear lack of documented proof of MARFA being suitable for use in safety assessments. SSM wishes that SKB clarifies how the verification of the MARFA code has been performed.

**Response:**

MARFA version 3.2.2 was used in SR-Site. Verification of MARFA version 3.2.2 is documented in the MARFA User's Manual R-09-56 (note erratum issued on 2013-04), Appendix C in TR-10-50, and the body of TR-10-50. An update to the Users Manual addressing version 3.2.3 is available as Posiva Working Report 2013-01. Testing of the underlying algorithms is documented in a peer-reviewed journal (Painter et al. 2008) article and in a peer-reviewed conference proceedings paper (Painter 2008). Results of additional testing of version 3.2.2 are summarized later in this response.

As has been pointed out by Robinson and Watson (2011), the MARFA User's Manual (R-09-56) contained errors in description of some of the test cases. Specifically, values of physical parameters for some of the tests cases were not consistent with the actual test case. An erratum has been issued to correct the errors (see also Posiva Working Report 2013-01). It is important to recognize that the errors only related to quoted values of some test parameters. The MARFA input and the input to the independent numerical calculations were fully consistent. The verifications tests described in R-09-56 are thus relevant tests of the proper working of the code.

The verification tests described in R-09-56 were designed to test major functionality of MARFA 3.2.2 that we anticipated would be used in SR-Site. All significant MARFA capability used in SR-Site was addressed in one or more Verification Tests. Table 1 summarizes the major capability probed in each test.

| Verification Test | Major Capability Tested |
|---|---|
| 1 | Advection, dispersion, diffusion into an infinite matrix with sorption, radioactive decay and in-growth. |
| 2 | Advection, dispersion, diffusion into a finite matrix with sorption, radioactive decay and in-growth. |
| 2a | Advection, dispersion, diffusion into a finite matrix with sorption, radioactive decay and in-growth, proper transfer of mass from one segment to the next in the pathway. |
| 3 | Advection, dispersion, diffusion into an infinite matrix with sorption, diffusion into a finite matrix with sorption, radioactive decay and in-growth, simultaneous representation of multiple sources and pathways. |
| 4 | Advection, dispersion, diffusion into an infinite matrix with sorption, radioactive decay and in-growth, changes in flow speed. |
| 5 | Advection, dispersion, diffusion into a finite matrix with sorption, radioactive decay and in-growth, changes in flow speed. |
| 5a | Advection, dispersion, diffusion into a finite matrix with sorption, radioactive decay and in-growth, changes in flow speed, proper transfer of mass from one segment to the next in the pathway. |
| 6 | Tests of same capabilities as Test 4 but for a different set of flow changes. |
| 7 | Advection, dispersion, diffusion into an infinite matrix with sorption, radioactive decay and in-growth, changes in flow speed. |

The report R-09-56 was released prior to final SR-Site parameter sets being available. Testing subsequent to release of R-09-56 is described in TR-10-50. Specifically, four direct comparisons between MARFA and the FARF code are provided in Appendix C of TR-10-50. Those four tests used the transport pathways that resulted in the largest radiological dose for the Q1 and Q3 release modes of the growing pinhole case. In addition, the tests used near-field releases calculated for the growing pinhole scenario instead of the hypothetical/presumed releases of R-09-56. The radionuclides Ra-226, I-129 and Cs-135 were considered in the tests. It should be noted that Ra-226 is the radionuclide that contributes the most to dose in SR-Site. I-129 and Cs-135 are important radionuclides in some variant cases. In addition to the tests shown in Appendix C of TR-10-50, both MARFA and FARF were used for the probabilistic central corrosion case. Although a direct comparison plotted on the same figure is not given in TR-10-50, agreement between the two codes can be verified by comparing the black dashed curve in Figure 4-5 (FARF) with the black solid curve of Figure 4-24 (MARFA). Note the probabilistic central corrosion case used 2800 realizations and 37 radionuclides and is the most

important far-field transport case in SR-Site. The conditions for that MARFA/FARF comparison are thus relevant for SR-Site, by definition.

Appendix A of this document provides results of four new tests of MARFA 3.2.2. Two of the new tests used the matrix diffusion model but span a wider range of matrix retention conditions than addressed in R-09-56. The strength of the radionuclide interaction with the rock matrix is quantified by the parameter $\kappa$, defined as $\kappa = \sqrt{D_{eff}\theta_m R_m}$ where $D_{eff}$ is the effective diffusion coefficient for the matrix, $\theta_m$ is the matrix porosity, and $R_m$ is the matrix retardation factor. Combining all realizations of the central corrosion case and all radioelements, the values of $\kappa$ for SR-Site range from about $10^{-5}$ m-yr$^{-1/2}$ for non-sorbing radioelements to about $10^{-2}$ m-yr$^{-1/2}$ for the most strongly sorbing radioelements. The $\kappa$ values used in R-09-56 are in the range $10^{-4}$ m-yr$^{-1/2}$ to 3 $10^{-4}$ m-yr$^{-1/2}$, consistent with those of the dominant dose contributor Ra-226. The new tests in Appendix A use $\kappa$ values that range from $10^{-6}$ m-yr$^{-1/2}$ to $10^{-2}$ m-yr$^{-1/2}$. As can be seen in Figures A-1 and A-2, MARFA compares quite well with the independent numerical calculations for both very strong and very weak matrix interactions.

That MARFA compares well with the independent numerical result for the situation of very weak matrix interaction is inconsistent with the findings of Robinson (2012) and Robinson and Watson (2011) who concluded that "systems where transport in the rock matrix are not dominant are not handled well" (Robinson 2012). That finding appears to be based on results in Figure 37 of Robinson and Watson (2011), which involved flow changes and weak matrix interaction. In their results, MARFA overestimates breakthrough following a flow change by at most a factor of two. Their conclusion about weak matrix interaction not being handled well is overly broad. It is clear from Figure A-1 and from Robinson and Watson's Figure 37 before the first flow change that weak matrix interaction is handled quite well in MARFA in steady-state flow fields. The factor of two discrepancy in Robinson and Watson's Figure 37 is caused by MARFA's handling of flow changes, not weak matrix interaction.

The MARFA algorithm for handling flow changes is approximate, as is fully acknowledged in R-09-56 and by Painter (2008). This approximate treatment of the flow changes is judged to be a minor consideration given the highly stylized and pessimistic scenarios used in the glacial scenarios in SR-Site. A discussion of the scenarios and an exploration of a more realistic treatment are summarized in Selroos et al. (2012). More importantly, the tests that involve flow changes in R-09-56 and the Robinson and Watson tests based on those tests are not representative of the SR-Site application of MARFA. Specifically, the SR-Site MARFA applications involve flow paths that are discretized into dozens of individual segments (hundreds of segments for most of the flow paths) while the test of Figure 37 of Robinson and Watson used only one segment. As is the case with many numerical methods, the MARFA approach for handling flow changes becomes more accurate as the flowpath is more finely discretized. Two of the new tests described in Appendix

A are designed to test MARFA's representation of the effect of flow changes in conditions more relevant to applications in SR-Site. The two tests consider a 300-year period where the flow rate is a factor of 50 higher than the nominal value. The duration and increase in flow is similar to that of the high-flow period following glacial retreat in SR-Site. The flowpath is discretized into 100 segments. The Peclet number is 10, the SR-Site value. One of the tests used non-sorbing radionulides, which respond very fast to flow changes and resulting in significant spikes in the breakthrough curves. The other test considered radionuclides with matrix retardation factors of 1000. As can be seen in Figures A-3 and A-4, the agreement between MARFA and the independent numerical result is reasonably good for both tests and much better than that shown in R-09-56. Given the results of those two tests, the highly stylized and pessimistic nature of the scenario used, and the post SR-Site analyses of a more realistic glacial scenarios of Selroos et al. (2012), it is SKB's position that the glacial scenarios in SR-Site are adequately represented by MARFA.

Robinson and Watson (2011) question MARFA's handling of the U238 decay chain. As discussed in Appendix B of this document, their example is not relevant to SR-Site because it does not include the direct source of U238 progeny radionuclides. Because of U-238's very long half-life, the secondary sources of U-238 progeny radionuclides from U-238 decay while in the far field are negligible compared with the direct releases from the near field into the far field. Based on results in Appendix B, we agree with Robinson (2012) who points out that the difficulty that MARFA has with the example in Section 4.6.5 of Robinson and Watson (2011) has negligible risk significance.

**SSM Question:** MARFA has a direct coupling (through ptv files) with the DFN results from ConnectFlow. SSM requests whether the stochastic rock properties in MARFA have been used, and how transport properties of individual segments in the ptv files have been determined. This is also requested in the report by Robinson (2012).

**Response:**

The MARFA 3.2 series has two major modes of operation depending on how the transport pathways are represented. In the stochastic pathway mode the flow-related properties of the transport pathway are stochastically simulated around a specified mean pathway within MARFA using the algorithm described by Painter and Cvetkovic (2005). In the deterministic pathway mode of MARFA, the properties of each segment on each segmented flowpath are specified as input. SR-Site used only the deterministic pathway mode of MARFA; the stochastic pathway mode was not used.

In SR-Site, the flowpath segments were read by MARFA from PTV files. The information read for each segment includes the advective travel time $t_w$, the transport resistance factor F, the segment length, and the rock type to which the segment belongs. Retention/sorption properties for each rock type were assigned through another file, as described in the MARFA User's Manual. It is noted that in some of the variant cases, the PTV files were modified from those produced by CONNECTFLOW. For example, flowpath segments corresponding to repository tunnels were removed from the CONNECTFLOW-generated PTV files for cases that neglected the advective delay in tunnels. The modified PTV files are contained in the data archive for the MARFA SR-Site runs.

Appendix C of TR-10-50 contains comparisons of MARFA to the code FARF. In that verification exercise, four combinations of flowpaths and radionuclides were used. Close agreement in calculated breakthrough was obtained in the comparison, with the only discernable difference being attributable to differences in temporal resolution. Those four MARFA model runs read flowpath segment information from the appropriate PTV file, while FARF read the global $t_w$ and F values from the corresponding PTB file, as described in TR-10-50. Note the PTB file contains one set of global flow-related transport properties for each pathway in the PTV file. That is, the PTB file is a summary of the PTV file. The verification exercise thus confirms not only that the transport solution in MARFA is correct for conditions relevant to SR-Site but also that MARFA's reading of PTV files is correct. In addition, the software comparisons confirm that MARFA's PTV-based dataflow and FARF's PTB-based dataflow are fully consistent. Moreover, the proper transfer of radionuclide near-field release data from the near-field code COMP23 to MARFA is confirmed.

MARFA's stochastic pathway representation discussed above refers to one strategy for capturing the effects of unresolved spatial heterogeneity. It was not used in SR-

Site and should not be confused with the computational strategy employed in SR-Site to address parametric uncertainties. The modeling cases described as "probabilistic calculations" in TR-10-50 used a sampling strategy to address parametric uncertainties. Details can be found in TR-10-50. The result of that sampling strategy is a set of transport realizations where each realization is a unique combination of sampled attributes including failed canister location, canister failure time, flowpath linking the failed canister location to locations of discharge points in the biosphere, and retention/sorption parameters of the far-field rock matrix. Because a similar sampling scheme is used in the near field, each transport-pathway realization also has an associated realization of the near-field releases to the far field.

When FARF was used for the probabilistic cases, FARF was executed for each transport realization independently. The results were then averaged to obtain the mean annual dose. When MARFA was used for the probabilistic cases, a different strategy was used. Specifically, all transport realizations were presented to MARFA simultaneously. Transport realizations from the set were then sampled internally within MARFA assuming each is equally probable, the same assumption used for the FARF calculations. Specifically, MARFA randomly selects one realizations from the set of equally probable realizations each time a particle representing a packet of radionuclide mass is launched. Stated differently, sampling to obtain a Monte Carlo estimate of the dose and sampling to resolve parametric uncertainty are intermingled. After dividing by the number of realizations and multiplying by the probability of a single failure, the result is a direct Monte Carlo estimate of the mean mass discharge into the biosphere. The result obtained this way is formally equivalent to first obtaining an estimate of mass discharge for each realization and then averaging the results.

MARFA was used for some probabilistic calculations of the central corrosion case. For those calculations, a new PTV file containing 2800 realizations of the transport pathway was created. Each pathway in the new PTV file is the CONNECTFLOW flowpath corresponding to one of the failure times listed in Table 4-1 of TR-10-50 but with a unique rocktype identifier. The flowpaths were modified to associate a unique rocktype identifier with each transport pathway but were otherwise extracted from the original CONNECTFLOW-generated PTV file. The unique rocktype identifier was necessary to associate one of the 2800 sets of sampled sorption/retention parameters with each flowpath. The PTV file for the MARFA probabilistic calculation of the central corrosion case is then composed of 2800 flowpaths representing 50 repetitions of each of the 56 flowpaths associated with the failure times of Table 4-1 but with a unique rocktype identifier for each flowpath. The PTV input file was then combined with a MARFA *source.dat* file with 2800 realizations of near-field release and a MARFA *rocktypes.dat* file with 2800 realizations of the matrix retention parameters. Details on the MARFA input protocol may be found in the Users Manual (TR-10-50 and Posiva Working Report 2013-01).

Although not explicitly addressed in the body of TR-10-50, results shown there make it possible to compare MARFA and FARF results for probabilistic calculation of the central corrosion case. Although a direct comparison plotted on the same figure is not given in TR-10-50, agreement between the two codes can be verified by comparing the black dashed curve in Figure 4-5 (FARF) with the black solid curve of Figure 4-24 (MARFA). Note the central corrosion case used 2800 realizations and 37 radionuclides and is the most important far-field transport case in SR-Site. The conditions for that MARFA/FARF comparison are thus relevant for SR-Site, by definition.

**SSM Question:** In the report by Little et al. (2012), a more complete explanation of the model presented in appendix I-2 in TR-10-50 is requested; for example, how is sorption of Ra-226 handled. SSM wishes that SKB provides this explanation.

**Response:**

The site-limited irreversible sorption model shown in Appendix I-2 was not used in SR-Site. The reversible sorption model of Appendix I-1 was used. As described in Section 4.5.6 of TR-10-50 and in the Main Report, the distribution coefficient for sorption onto bentonite colloids for each radioelement was taken to be the same as that radioelement's distribution coefficient for sorption onto the bentonite buffer. We note that due to an editing error the captions in Figures 4-26 and 4-27 of TR-10-50 incorrectly imply that colloid-facilitated transport was applied only for actinides and transition metals. The model was actually applied to all radionuclides, but has no effect on non-sorbing radioelements.

## References

Painter S, Mancillas J, 2009. MARFA version 3.2.2 user's manual: migration analysis of radionuclides in the far field. SKB R-09-56, Svensk Kärnbränslehantering AB.

Painter S, Mancillas J, 2013. MARFA version 3.2.3 user's manual: migration analysis of radionuclides in the far field. Posiva Working Report 2013-01, Posiva Oy.

Painter S, Cvetkovic V, 2005. Upscaling discrete fracture network simulations: An alternative to continuum transport models. Water Resources Research 41(2).

Painter S, Cvetkovic V, Mancillas J, Pensado O. 2008. Time domain particle tracking methods for simulating transport with retention and first-order transformation. Water Resources Research 44(1).

Painter S, 2008. Accommodating Transient Velocities in Time-Domain Particle Tracking Algorithms of Radionuclide Transport, Proceedings of the 12th International High-Level Radioactive Waste Management Conference (IHLRWM); 7–11 September 2008; Las Vegas, American Nuclear Society (CD ROM).

Robinson P, Watson C, 2011. Handling interfaces and time-varying properties of radionuclide transport models, SSM 2011:11, Strålsäkerhetsmyndigheten.

Robinson P. 2012. Review of the MARFA code, SSM 2012:62, Strålsäkerhetsmyndigheten.

Selroos JO, Cheng H, Painter S, Vidstrand P. 2012. Radionuclide transport during glacial cycles: Comparison of two approaches for representing flow transients. Physics and Chemistry of the Earth, Parts A/B/C.

SKB, 2010. Radionuclide transport report for the safety assessment SR-Site. SKB TR-10-50, Svensk Kärnbränslehantering AB.

## Appendix A: Additional Testing of MARFA 3.2.2

This Appendix provides results of four new tests of MARFA 3.2.2. Two of the new tests used the matrix diffusion model but span a wider range of matrix retention conditions than addressed in R-09-56. The other two tests are designed to test MARFA's representation of the effect of flow changes in conditions similar to those of the SR-Site glacial scenarios.

*A.1 Tests with a wider range of matrix interactions.*

The strength of the radionuclide interaction with the rock matrix is quantified by the parameter $\kappa$, defined as $\kappa = \sqrt{D_{eff}\theta_m R_m}$ where $D_{eff}$ is the effective diffusion coefficient for the matrix, $\theta_m$ is the matrix porosity, and $R_m$ is the matrix retardation factor. Combining all realizations of the central corrosion case and all radioelements, the values of $\kappa$ for SR-Site range from about $10^{-5}$ m-yr$^{-1/2}$ for non-sorbing radioelements to about $10^{-2}$ m-yr$^{-1/2}$ for the most strongly sorbing radioelements. The $\kappa$ values used in R-09-56 are in the range $10^{-4}$ m-yr$^{-1/2}$ to 3 $10^{-4}$ m-yr$^{-1/2}$, consistent with those of the dominant dose contributor Ra-226. Regression testing of MARFA 3.2.2 using the new verification tests that span a wider range of retention strengths is summarized in Figures A-1 and A-2.

Verification Test 2b is identical to Verification Test 2 (two-member chain, single segment, constant flow, limited diffusion model, exponentially decaying source of species A) except that in Test 2b the $\kappa$ values are 3.16 $10^{-5}$ m/yr$^{1/2}$ and $10^{-6}$ m/yr$^{1/2}$ for species A and B, respectively, and the half-life is $10^5$ yrs for both species. The $\kappa$ values correspond to the following physical parameters: $D_{eff} = 10^{-9}$ m$^2$/yr, $\theta_m$ of 0.001, and $R_m$ of 1000 for species A and 1 for species B. Results of the comparison with an independent numerical solution are shown in Figure A-1. The agreement is good over a wide range, which is compelling evidence that MARFA can adequately represent transport with very weak matrix interaction. It is important to note that the $\kappa$ value of $10^{-6}$ m-yr$^{-1/2}$ for species B is smaller than the smallest value used in SR-Site.

Verification Test 2c is identical to Test 2a in the representation of the pathway (two-member chain, ten segments, constant flow, limited diffusion model). The retention parameters are $D_{eff} = 10^{-7}$ m$^2$/yr, $\theta_m$ of 0.1, and $R_m$ of $10^5$ for both species. The size of the accessible matrix region is 4.75 cm, and the dispersivity is 10 m in Test 2c. The half-live is $10^6$ yrs for both species. The $\kappa$ value for both species is 0.0316 m-yr$^{-1/2}$. Results of Test 2c are shown in Figure A-2. The agreement is good, which indicates that MARFA is able to correctly represent transport for very strongly sorbing radionuclides. The breakthrough curves are somewhat noisier in this test compared with other tests because few of the released particles survive with the strong matrix retention. Ten million particles were used in Test 2c.

*A.2 Tests with flow changes representative of SR-Site conditions*

Two new variants of the original Verification Test 6 are summarized here. These two new tests consider a 300-year period where the flow rate is a factor of 50 higher than the initial value. Specifically, the flow rate is 1 m/yr up to year 2000, 50 m/yr between year 2000 to year 2300, then 1 m/yr after year 2300. The duration and increase in flow is similar to that of the high-flow period following glacial retreat in SR-Site. The flowpath is 500 m long and discretized into 100 segments. The dispersivity is 50 m, which corresponds to a Peclet number of 10. The fracture half-aperture is 0.1 mm. Diffusion is into a 10 cm matrix region, with $D_{eff} = 10^{-8}$ $m^2$/yr and $\theta_m$ of 0.1. Both species have a decay constant of $10^{-4}$ $yr^{-1}$.

One of the new tests, denoted Test 6a, considers radionuclides with matrix retardation factors of 1000. The other test, Test 6b, uses non-sorbing radionulides, which respond very fast to flow changes and resulting in significant spikes in the breakthrough curves.

Results of Verification Tests 6a and 6b are shown in Figures A-3 and A-4 respectively. Although minor differences between the MARFA result and the independent numerical solution are apparent, reasonably good agreement is seen over a wide range. The agreement is better than that shown in the single-segment test of R-09-56. It is emphasized that the conditions of Test 6a and Test 6b are quite similar to those of SR-Site. Given the stylized and pessimistic nature of the glacial modeling cases in SR-Site, the quality of the MARFA solution is judged to be acceptable.

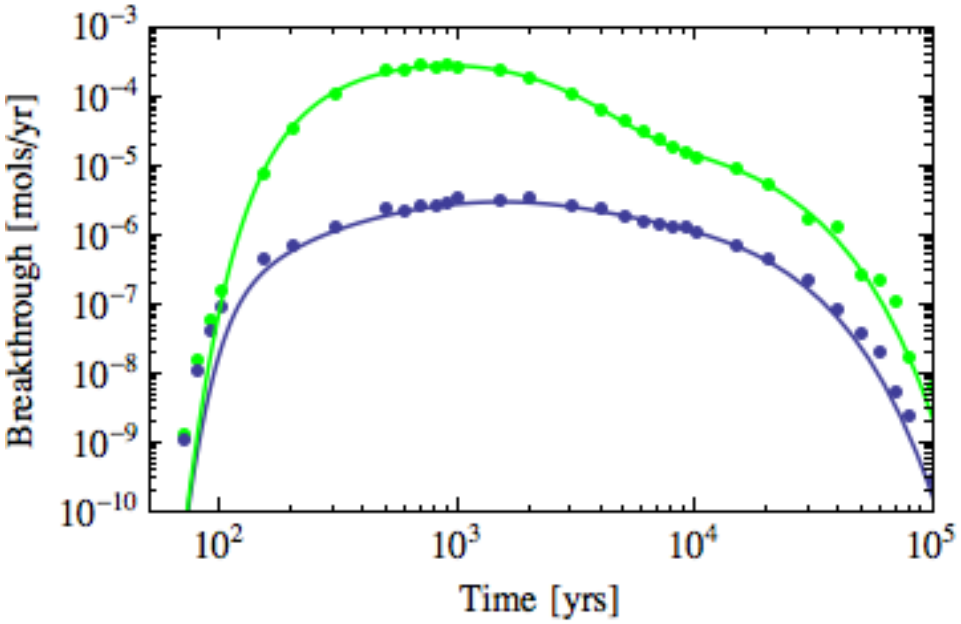


***Figure A-1.*** *MARFA version 3.2.2 results for the new Verification Test 2b, which is designed to test the situation of very weak matrix interaction. Results for species A are shown in green. Results for species B are shown in dark blue. The individual data points are MARFA 3.2.2 results. The curves are the results of an independent numerical calculation using the same mathematical model.*

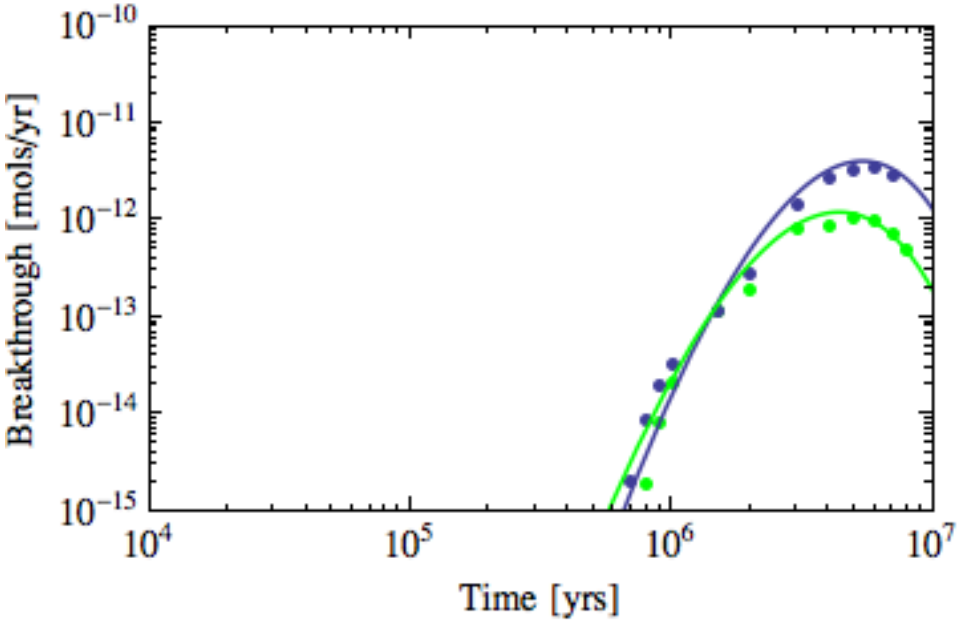


***Figure A-2.*** *MARFA version 3.2.2 results for the new Verification Test 2c, which is designed to test the situation of strong matrix interaction. Results for species A are shown in green. Results for species B are shown in dark blue. The individual data points are MARFA 3.2.2 results. The curves are the results of an independent numerical calculation using the same mathematical model.*

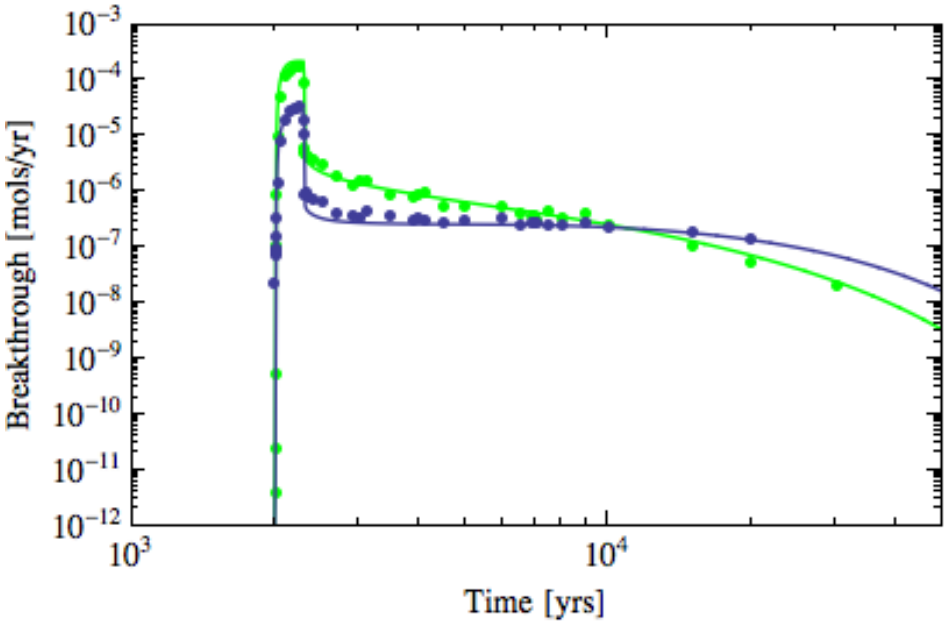


***Figure A-3.*** *MARFA version 3.2.2 results for the new Verification Test 6a, which addresses transport effects of flow changes in conditions similar to those of the SR-Site variant cases involving flow changes. Results for species A are shown in green. Results for species B are shown in dark blue. The individual data points are MARFA 3.2.2 results. The curves are the results of an independent numerical calculation using the same mathematical model. The two radionuclides in this example are moderately sorbing (matrix retardation factor of 1000).*

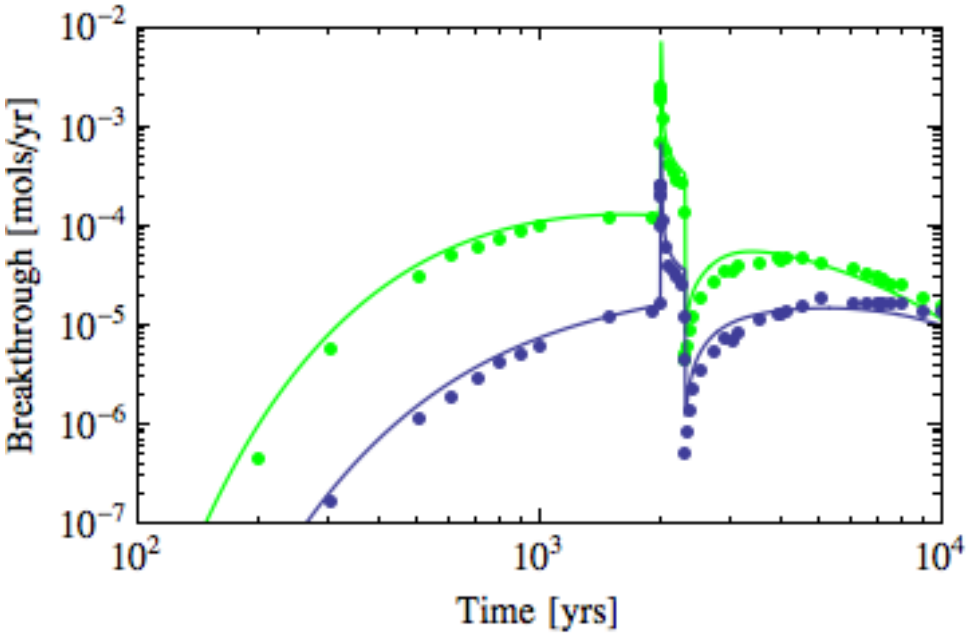


***Figure A-4.*** *MARFA version 3.2.2 results for the new Verification Test 6b, which addresses transport effects of flow changes in conditions similar to those of the SR-Site variant cases involving flow changes. Results for species A are shown in green. Results for species B are shown in dark blue. The individual data points are MARFA 3.2.2 results. The curves are the results of an independent numerical calculation using the same mathematical model. The two radionuclides in this example are non-sorbing and thus respond very quickly to flow changes.*

## Appendix B: Transport of the U-238 Decay Chain

Robinson and Watson [2011] question MARFA's handling of realistic decay chains. Their comment is based on results in their Section 4.6.5, which considered the transport of the U-238 decay chain. In their example, U-238 was released into the transport pathway with no direct release of progeny radionuclides. With no direct release of progeny radionuclides, the only source of U-234, Th-230, Ra-226 and Pb-210 mass is through decay of U-238 and in-growth of the progeny radionuclides. Because the half-life of U-238 is extremely long (more than 4 billions years) a very small fraction of the released U-238 particles decay while in the transport pathway. It is estimated that approximately 150 U-238 particles would have decayed while en route in their example, which is orders of magnitude too few particles to obtain a reliable estimate of the progeny mass breakthrough. Thus, the cause of the unreliable breakthrough curves is a combination of the very long-lived radionuclide and no direct source of other radionuclides. It is not caused by short-lived daughter nuclides, as stated by Robinson and Watson.

Although this example does illuminate a limitation of previous MARFA version when representing decay chains containing a nuclide with a very long half-life, the example has no relevance to SR-Site. Specifically, the radionuclide releases from the engineered barrier systems, the input to MARFA, typically contains a direct source of the daughter products, which are generated in the reactor and by U238 decay prior to release to the far field. This direct source greatly overwhelms any indirect source created by decay of the long-lived U-238 while in transit in the geosphere. Indeed, referring to Figure 4-34 of TR-10-50, it can be seen that Ra-226 is the radionuclide with *largest* release from the near field. This direct release overwhelms any indirect source of Ra-226 through the U-238 decay chain, as demonstrated in Figure B-1. Thus, the example of Robinson and Watson, which ignores the direct release of the U-238 progeny has no relevance to SR-Site.

Starting with Versions 3.2.3 and 3.3.1, an optional particle splitting algorithm is available in MARFA. This algorithm makes it possible to get reliable estimates of breakthrough curves for decay chains with very long half-lives. Results for the Robinson and Watson example are shown in Posiva Working Report 2013-01. In Figure B-1, this new capability is used to demonstrate that the indirect source of Ra-226 through the U-238 decay chain is negligible compared with the direct release of Ra-226 from the near field.

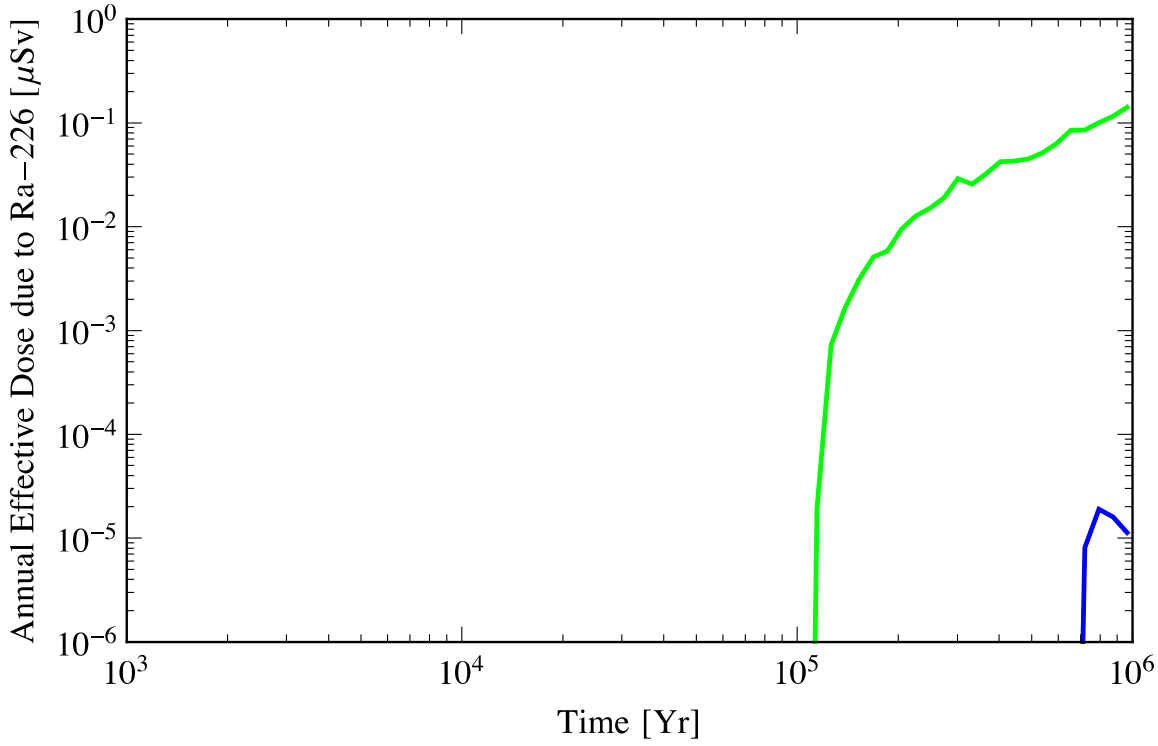


***Figure B-1.*** *Far-field annual effective dose due to Ra-226 release from the near field (green) compared with that due to Ra-226 in-growth from U-238 while in the far field (blue). MARFA versions prior to Version 3.2.3 had difficulty obtaining statistically reliable estimates of the breakthrough curve for Ra-226 due to in-growth from U-238 in the far field (Robinson and Watson, 2011). New particle-splitting capability added in Version 3.2.3 make it possible to obtain reliable estimates and were used for the blue curve. That the dose due to direct release is nearly four orders of magnitude larger than the dose due to in-growth clearly demonstrates that Version 3.2.2 limitations in handling the U-238 decay chain have no significant effect on the SR-Site results.*